Int. J. Nano Dimens., 10 (3): 230-241, Summer 2019

ORIGINAL ARTICLE

Synthesis and electrochemical studies on Cu-TiO_2 thin films deposited by spray pyrolysis technique for sensing Uric acid

Arunananthan Mathi Vathani [1], Selvaraj Dhanalakshmi [2], Natarajan Prithivikumaran [1,]*

[1]*Department of Physics, V.H.N. Senthikumara Nadar College, Virudhunagar, India.*
[2]*Department of Chemistry, V.H.N. Senthikumara Nadar College, Virudhunagar, India.*

Recived 23 January 2019, revised 01 April 2019, accepted 12 April 2019, available online 13 April 2019

Abstract
In this study, we report an effective uric acid (UA) electrochemical biosensor using Cu-TiO_2 electrode. UA is a biomedical compound that plays a vital role in human metabolism. The abnormal level of UA leads to several diseases. TiO_2 and Cu-TiO_2 with various concentrations were deposited on glass substrates by spray pyrolysis technique. X-ray diffraction analysis shows that all the films are in anatase phase with tetragonal structure and confirm the incorporation of Cu ions into TiO_2 lattice. The morphology and chemical composition of TiO_2 and Cu-TiO_2 were characterized by scanning electron microscopy (SEM) and energy-dispersive x-ray spectroscopy (EDS). These studies reveal that the aggregation of particles occurs due to doping and confirm the presence of Cu. The optical analysis was studied by UV-Vis absorption and photoluminescence spectroscopy, which indicates the band gap changes, shift in absorption peak and defects. Cyclic voltammetry (CV) was used to analyse the performance of the Cu-TiO_2 as the electrochemical biosensor. Cu-TiO_2 electrochemical biosensor exhibits good sensitivity, linearity and high stability for the detection of UA.

Keywords: *Cu- TiO_2; Electrochemical Studies; Sensing; Spray Pyrolysis; Thin Films; Uric Acid.*

How to cite this article
Vathani AM, Dhanalakshmi S, Prithivikumaran N. Synthesis and electrochemical studies on Cu-TiO_2 thin films deposited by spray pyrolysis technique for sensing Uric acid. Int. J. Nano Dimens., 2019; 10 (3): 230-241.

INTRODUCTION

Uric acid (2,6,8-trihydroxypurine, UA) and other oxy-purines are the principal final products of purine metabolism in the human body [1]. UA is biomedically important compound that plays a vital role in human metabolism [2]. Abnormal level of UA in human body causes several diseases including gout, hyperuricemia, lesch-nyan disease, cardiovascular and chronic renal sickness [3-6]. Several methods can be applied to determine the UA concentration including high performance liquid chromatography [7], amperometric [8], fluorometric enzymatic method [9] and electrochemical analysis [6]. In recent years the electrochemical analysis have gained attention in the investigation of important biological molecules and drugs because of their simplicity, cost effectiveness, easy handling and highly sensitive compared to other methods [10]. The objective of the work is to fabricate a metal doped semiconductor electrode material for electrochemical biosensor to sense UA.

Titanium dioxide (TiO_2) has extreme attentions as a potential semiconductor material with wide range of technological applications [11]. It is a widely used semiconductor material for various applications such as dye-sensitized solar cells, water photoelectrolysis, photocatalysis, gas sensors, chemical oxygen detection (COD) sensor and biosensor [12]. Environmental friendly TiO_2 thin films got interest in the field of biosensor due to its good biocompatibility, large surface area and good surface, structural, physical, chemical and optical properties. The immobilizing amount of enzymes, activity of immobilized enzymes and conductivity are the key factors for the sensitivity of biosensors [13-14]. Many researchers have

* Corresponding Author Email: *prithivikumaran@vhnsnc.edu.in*

made the synthesis and modification of TiO_2 for enhancing the electrochemical performance. The modification of TiO_2 with doping enhances the charge transfer rate between the electrolyte and the electrode which also enhances the detection performances of the biosensors. Cu^{2+} causes more effective doping with titanium oxide since ionic radii of Cu^{2+} (0.87 Å) and Ti^{4+} (0.75 Å) are similar to each other. Hence Cu^{2+} ion can easily substitute Ti^{4+} ion in TiO_2 lattice without destroying the crystal structure, thereby stabilizing the anatase phase [15]. Cu doped TiO_2 shows fast electron transfer rate than TiO_2 electrode, hence the sensing property of TiO_2 was found to be enhanced by doping with metals.

Semiconductors in the form of thin films find greater technological importance because of their variety of advantages over bulk crystals [16]. TiO_2 thin films were fabricated by many methods including molecular beam epitaxy, spin coating, electro deposition, RF-magnetron sputtering, pulsed laser deposition (PLD), metal–organic chemical vapour deposition (MOCVD) and spray pyrolysis. Among these spray pyrolysis is a cost effective, simple and efficient technique. This technique has the capability to produce large surface area, high quality adherent films with uniformity, easiness of doping, operates at moderate temperatures (100-500˚C) that opens the possibility of wide variety of substrates, control of thickness, variation of film composition along with thickness and possibility of multilayer deposition [17-18].

In the present work, Cu doped TiO_2 (Cu-TiO_2) thin film electrode material was synthesized by spray pyrolysis technique. The concentration of Cu dopant in TiO_2 thin film was varied in order to optimize the film. Its structural, morphological, optical and electrochemical properties were analyzed and discussed in detail. The linearity and stability of the Cu-TiO_2 thin film electrode was reported. Also, Cu-TiO_2 electrode biosensor was constructed and the sensing performance of UA was studied.

CHEMICALS AND METHODS

The chemicals used for the preparation of TiO_2 and Cu-TiO_2 thin films were titanium tetra-isopropoxide (TTIP, $Ti\{OCH(CH_3)_2\}_4$, 97%), ethanol (C_2H_5OH, 99.9%), acetyl acetone (AcAc, $CH_3COCH_2COCH_3$, 98%), copper acetate dehydrate ($C_4H_{10}CuO_6$, 97%) and uric acid ($C_5H_4N_4O_3$, 99%). All the chemicals were bought in analytical grade and used without further purification.

Preparation of precursor solution and Fabrication of TiO_2 and Cu-TiO_2 Thin films

TiO_2 and Cu-TiO_2 thin films were deposited on finely cleaned glass slides by spray pyrolysis technique. Titanium tetra isopropoxide (TTIP) was the Ti precursor material and copper acetate was the material for doping copper. To prepare the solution to make TiO_2 films ethanol was mixed with the TTIP and stirred for 10 minutes and with that acetyl acetone (AcAc) was added as a stabilizer. Then ethanol was added again and stirred for an hour. Here the molar ratio of TTIP, ethanol and AcAc was maintained as 1 : 10 : 1. The prepared solution was sprayed onto well cleaned glass substrate with air as carrier gas, at a substrate temperature of 350 ˚C, spray rate of 4ml/min, pressure of 1 bar keeping the nozzle to substrate distance as 15cm. For uniformity in coatings, the spray head was allowed to move in the X–Y plane using the microcontroller. TiO_2 solution was sprayed for one minute over the glass slide and then the film was put into the muffle furnace for 10 minutes for annealing at 350 °C. This was considered as one coating. The similar process was followed up to 10 coatings. After that the TiO_2 thin film was post annealed at 500 ˚C for one hour. For the preparation of Cu-TiO_2 thin films copper acetate dihydrate was taken as copper source. To prepare Cu-TiO_2 precursor solution, the procedure detailed above to prepare TiO_2 precursor solution was followed and copper acetate was added finally and stirred again for one hour. The coating procedure is same as mentioned above. In order to optimize the optical, structural, surface and electrochemical properties of Cu-TiO_2 films, copper acetate of various concentrations ie., 0.025Wt%, 0.05 Wt%, 0.1 Wt% and 0.5 Wt% were added to the mixture to get four different Cu-TiO_2 thin film samples.

Characterization

The structural study was done using XRD technique by XPERT-PRO diffractometer which was operated at 40 KV and 30 mA using Cukα radiation of wavelength 1.5406 Å. The surface morphology (SEM) and elemental analysis of the TiO_2 and Cu-TiO_2 thin films were studied using ZEISS and VEGA3 TESCON scanning electron microscope. UV-Vis spectroscopic measurements of the films

were carried out by using SHIMADZU UV-Vis 1800 Spectrophotometer. Photoluminescence (PL) spectra were obtained using SHIMADZU RF-6000 Series PL spectrophotometer. Electrochemical analysis was carried out using CHI604E electrochemical work station.

RESULT AND DISCUSSION

Structural Analysis

X- ray diffraction patterns obtained for TiO_2 and different concentration of Cu-TiO_2 thin films are shown in Fig. 1(a). The films are polycrystalline in nature and well fitted with the tetragonal crystal structure and the thin films have dominantly anatase crystalline phase and low intensely rutile crystalline phase matched with JCPDS card no 21-1272. For TiO_2 thin film the diffraction peaks of anatase phase with the orientations of (1 0 1), (0 0 4), (1 0 5), (2 0 0) and (2 1 3) and of rutile phase at (211) and (320) are present. For 0.025Wt% Cu-TiO_2 thin film the anatase phase peak intensity slightly increases and rutile phase disappears which may be due to very low concentration of copper. As the concentration of Cu^{2+} is increased to 0.05Wt%, the intensity of anatase peaks gradually increased and rutile peaks reappear, which may be due to the incorporation or replacement of Cu^{2+} atoms into TiO_2 lattice. It indicates the better crystallinity of the film [19]. At 0.1Wt% of Cu- TiO_2 film, the intensity of anatase peaks was higher than that of TiO_2 thin film but lesser than that of 0.05Wt% of Cu- TiO_2 film. Further increase in Cu^{2+} concentration to 0.5Wt% the anatase peaks become weak which may be due to the

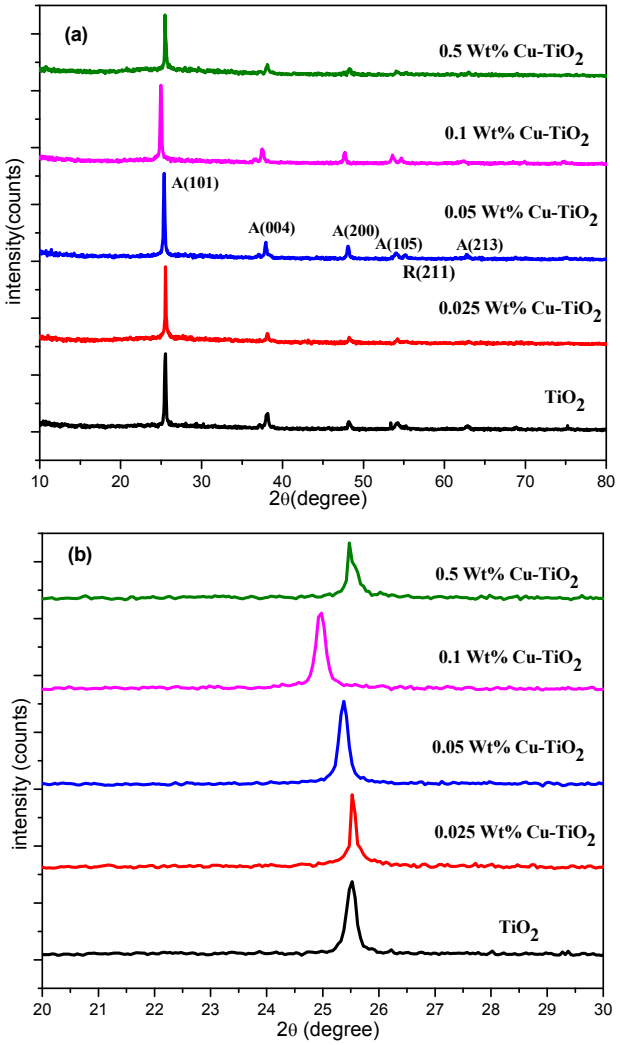

Fig. 1. (a) XRD pattern of TiO_2 and different concentration of Cu-TiO_2 thin films (b) Peak shift of Dominant peak.

reorientation effect [20-21] and also rutile phase disappears again. The similar result was observed for Sn doped TiO_2 thin films [22]. Fig. 1(b) reveals that the 0.025Wt%, 0.05Wt% and 0.1Wt% Cu-TiO_2 diffraction peak positions are slightly shifted towards the left compared to that of TiO_2 film. This shift refers to the incorporation or replacement of Cu^{2+} ions into the anatase TiO_2. Thus addition of dopant transforms the degree of phase (2θ) of the TiO_2 thin films and the transformation depends upon the Cu^{2+} concentrations [23].

The average crystallite sizes of the TiO_2 thin films were calculated by Scherrer's formula,

$$D = \frac{K\lambda}{\beta cos\theta} \text{ (nm)} \quad (1)$$

where K=0.94 - shape factor, λ - x-ray wavelength of Cukα radiation, θ - Bragg's angle and β - full width at half maximum of the peak. The average crystalline size of the synthesized TiO_2 film was 31.31nm as calculated from equation 1. The crystalline size increases when Cu^{2+} ions is added upto 0.05Wt% which may be due to replacement of Ti ions but further addition of Cu^{2+} ions decreases the crystalline size of the film which may be due to higher concentration.

The microstrain was calculated using the relation,

$$\varepsilon = \frac{\beta cos\theta}{4} \quad (2)$$

The values of Dislocation density (δ) were calculated using the formula,

$$\delta = \frac{1}{D^2} \text{ (lines/m}^2\text{)} \quad (3)$$

The strain and dislocation density decrease with the doping and it can be attributed to the incorporation of Cu ions into TiO_2 and difference between the ionic radius of Cu^{2+} and Ti^{4+} [19]. 0.05wt% Cu-TiO_2 film has better crystallinity, as the average crystalline size of it was larger and the dislocation density was lowest for it.

Morphological Analysis

Figs. 2(a) & (b) shows the surface morphology with 1kX magnification of TiO_2 and 0.05Wt% Cu-TiO_2 thin films coated on microscopic glass slides. The SEM micrograph of TiO_2 thin film depicts that the particles were fine spherical in shape and distributed all over the substrate. SEM image of 0.05Wt% Cu-TiO_2 thin film illustrates the agglomeration of the particles. Fig. 2 (c) shows the elemental analysis (EDX image) of 0.05Wt% Cu-TiO_2 thin film. It shows the presence of copper, titanium and oxygen in the sample. The absence of other elements indicates the purity of the film. The presence of copper peak from the analysis also reveals that the Cu^{2+} ions are incorporated in Ti^{4+} lattice sites [24].

Optical Analysis

UV-Vis spectroscopy analysis

The UV-Vis absorption spectra of the TiO_2 and Cu-TiO_2 thin films are shown in Fig. 3 (a). It shows the absorption is maximum for 0.05Wt% Cu-TiO_2 thin film. The optical band gap (Eg) values for the TiO_2 and Cu-TiO_2 films were calculated using the Tauc's relation,

$$(\alpha\, hv) = A(hv - E_g)^n \quad (4)$$

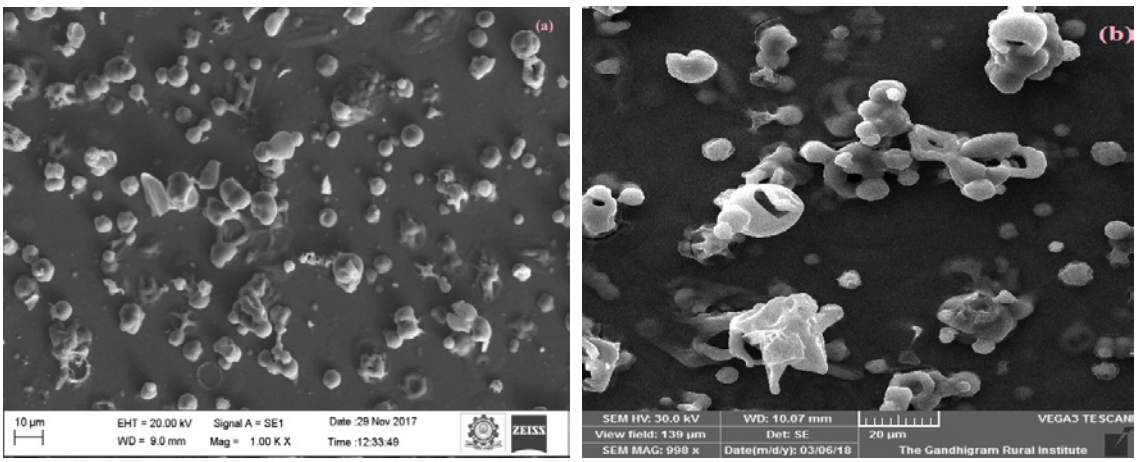

Fig. 2 (a) & (b). SEM images of TiO_2 and 0.05 Wt% of Cu-TiO_2 thin films and EDX image of 0.05 Wt% of Cu-TiO_2 thin films.

Where α is absorption coefficient, v is light frequency, h is Planck's constant, A is proportionality constant, E_g is band gap energy and there exponent n depends on type of transition. For a direct-allowed transition $n = 2$, for an indirect-allowed transition $n = 1/2$ and for an indirect forbidden transition $n = 3/2$. The obtained band gap values for TiO_2 and Cu-TiO_2 thin films from Fig. 3(b) are tabulated in Table 2. Anatase exhibits an indirect band gap that is smaller than its direct band gap [25]. The difference in band gap value may be attributed due to the morphological change and the improvement of crystallinity of anatase phase [26]. The band gap values shown in Table 2 agree well with XRD results which denote the quantum confinement effect [27]. In the UV-Vis absorption spectra, a notable shift to a higher wavelength occurs for 0.1Wt% and 0.05Wt% Cu-TiO_2 thin film when compared to TiO_2 film. It attributes to the incorporation of Cu^{2+} ions into Ti^{4+}

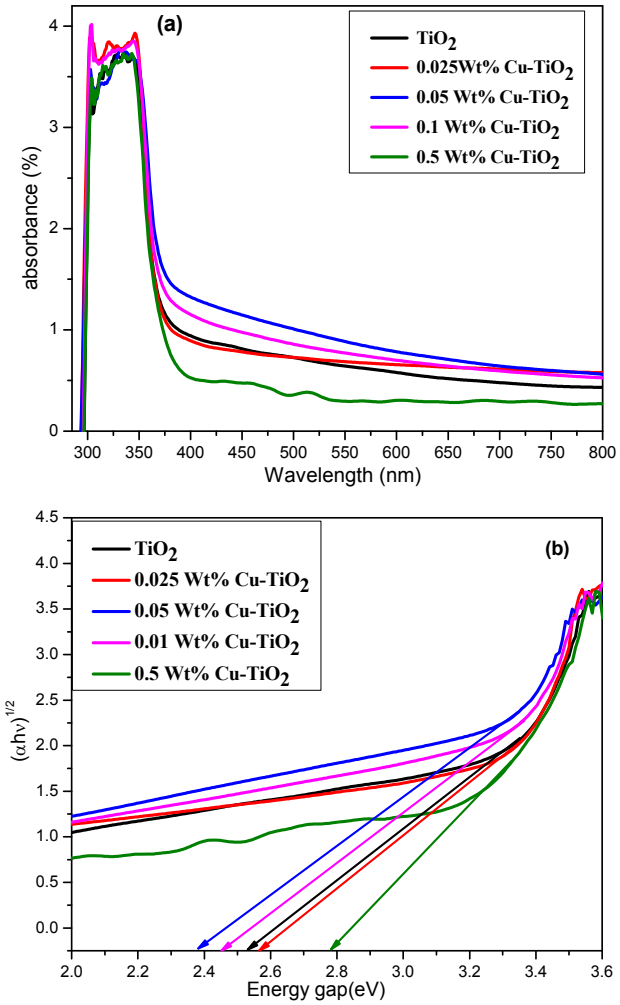

Fig. 3 (a) & (b). absorption & optical band gap spectra of TiO_2 and different concentration of Cu-TiO_2 thin films.

Table 1. Average crystalline size, Strain and Dislocation density values of the TiO_2 and different concentration of Cu-TiO_2 thin films.

Sample	Average crystalline size (nm)	Strain	Dislocation density (lines/m^2)
TiO_2	31.3113	0.0707	1.0199E+15
0.025wt% Cu-TiO_2	33.8231	0.0597	8.7412E+14
0.05wt% Cu-TiO_2	37.0746	0.0614	7.2752E+14
0.1wt% Cu- TiO_2	33.6692	0.0663	8.8213E+14
0.5wt% Cu-TiO_2	32.9363	0.0638	9.2182E+14

ions. It lowers the optical band gap of Cu-TiO_2 thin film by increasing its absorption band to visible region [28].

Photoluminescence Analysis

Photoluminescence (PL) spectrum of TiO_2 and different concentration of Cu-TiO_2 thin films are shown in Fig. 4. The violet emission peak obtained at 404 nm (3.07 eV) for TiO_2 film and at 391nm (3.16 eV) for Cu-TiO_2 thin films. Compared to TiO_2 film, the emission band was blue shifted for Cu-TiO_2 thin films. The blue shift of the PL peak was due to Cu doping [29]. The emission peak at 391nm might be due to luminescent centers, such as nano crystals and defects in the film [30]. The change of defect states on the shallow level of the film surface leads to variation in the PL intensity [31]. It is noted that, 0.05Wt% Cu-TiO_2 sample has the lowest intensity of the PL emission peaks, which indicates that the defect is less for the corresponding sample compared to the other samples. This is also confirmed by the XRD results which show that the dislocation density was lowest for 0.05 Wt% Cu-TiO_2 sample.

Table 2. Band gap values for the TiO_2 and different concentration of Cu-TiO_2 thin films.

Sample	Band gap(eV)
TiO_2	2.537
0.025 Wt% Cu- TiO_2	2.576
0.05wt% Cu-TiO_2	2.384
0.1wt% Cu- TiO_2	2.455
0.5wt% Cu-TiO_2	2.786

Electrochemical analysis

The electrochemical analysis with three electrode cell was carried out by using Ag/ AgCl (KCl) as reference electrode, glassy carbon electrode (GCE) as counter electrode and TiO_2 and Cu-TiO_2 thin film as working electrode, separately. 0.1M Phosphate buffer solution (PBS) with pH 7 was the electrolyte. In the present work, the electrochemical study was carried out for 0.05Wt% Cu-TiO_2 thin film along with TiO_2 film, as it has better crystallinity, lower optical band gap and lesser crystal defects.

Fig. 5(a) shows the cyclic voltammetry (CV) sweep plots of 0.05Wt% Cu-TiO_2 electrode at the scan rates of 50 mV/s, 75 mV/s, 100 mV/s and 150 mV/s. The anodic peak potentials (E_{pa}) and cathodic peak potentials (E_{pc}) for 0.05Wt% Cu-TiO_2

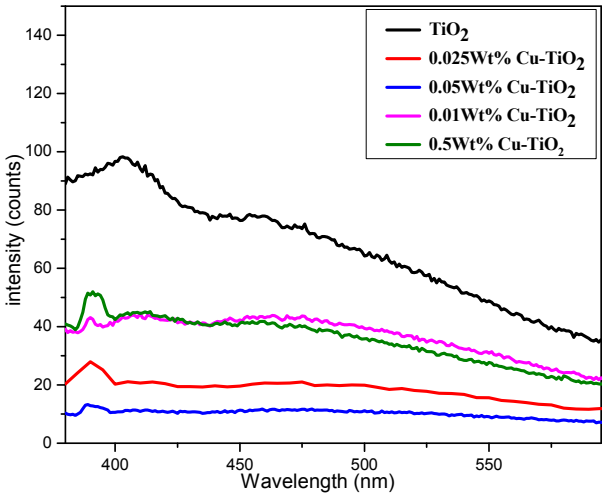

Fig. 4. Photoluminescence spectrum of TiO_2 and different concentration of Cu-TiO_2 thin films.

Table 3. anodic and cathodic peak potential (E_{pa}, E_{pc}) & anodic and cathodic peak current (I_{pa}, I_{pc}) of TiO_2 and 0.05 Wt% Cu-TiO_2 electrode.

Sample	Scan rate (mV/s)	E_{pa}	E_{pc}	I_{pa}	I_{pc}
TiO_2	150	0.0915	0.0646	3.34E-06	-3.26E-06
0.05 Wt% Cu- TiO_2	50	0.0514	0.0474	9.09E-07	-8.74E-07
	75	0.0546	0.0471	1.74E-06	-1.70E-06
	100	0.0553	0.0469	2.20E-06	-2.14E-06
	150	0.0563	0.0468	3.46E-06	-3.47E-06

electrode with various scan rates are shown in Table 3. It was observed that while increasing the scan rate, the anodic peak potentials shift towards higher potential and cathodic peak potentials shift towards lower potential which recommends the surface diffusion controlled and quasi reversible process [32]. The anodic peak current (I_{pa}) and cathodic peak current (I_{pc}) for 0.05Wt% Cu- TiO_2 electrode for various scan rates are obtained from the Fig. 5(a) and given in Table 3.

It was noted that the anodic current increased and cathodic current decreased with increase in scan rate from 50mV/s to 150mV/s. The comparison between CV sweep plot for TiO_2 and 0.05Wt% Cu-TiO_2 electrode at the scan rates of 150 mV/s was shown in Fig. 5(b). It was noted that the anodic and cathodic peak potential shifts towards lower potential for 0.05Wt% Cu-TiO_2 electrode due to doping effect. Similar report for anodic and cathodic peak potential shift was reported for TiO_2-NTAs and carbon doped TiO_2- NTAs [33]. 0.05Wt% Cu-TiO_2 electrode has high anodic current (I_{pa}) and cathodic current (I_{pc}) compared to TiO_2 electrode at 150mV/s. It shows that the electron transfer rate in Cu-TiO_2 is quicker than that of the TiO_2 electrode. Doping of Cu^{2+} ions into TiO_2 induces more oxygen vacancies into TiO_2.lattice [34]. Zhenguang shen *et al.*, reported that oxygen vacancies would bound electrons as free carriers and they introduce the donor level between the conduction and valance bands which would result in increased conductivity for semiconductor oxides [35]. The higher direct

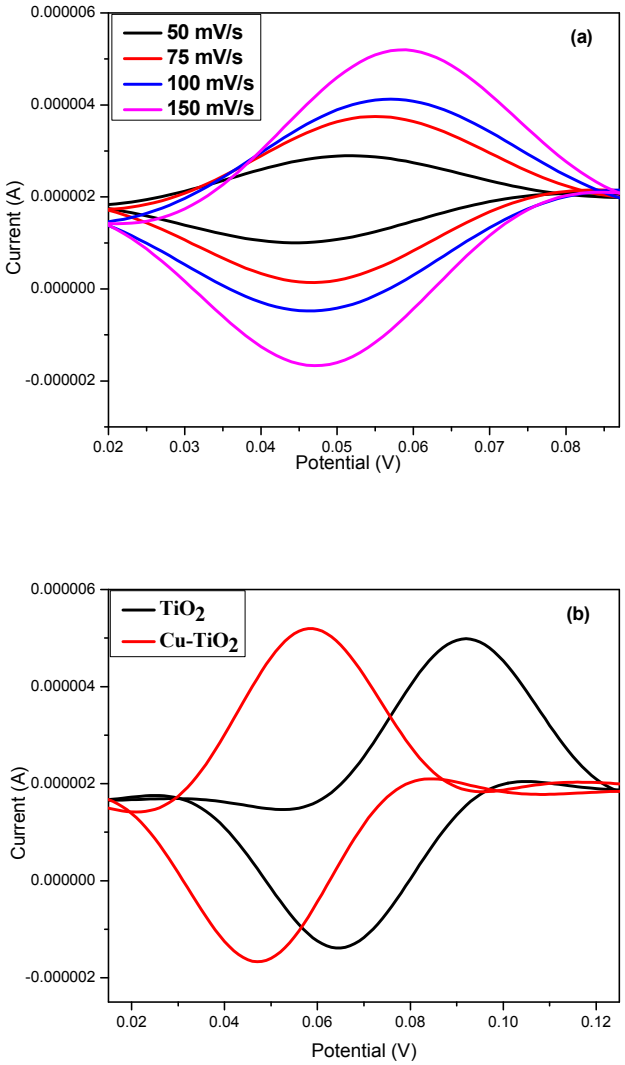

Fig. 5 (a). CV plot for Cu-TiO_2 electrode at various scan rates and (b) comparison of sweep plots of TiO_2 and Cu-TiO_2 electrodes at scan rate of 150 mV/s.

electron transfer between the electrode surface and 0.05Wt% Cu-TiO_2 electrode gives rise to enhanced voltammetric response [36].

The correlation between scan rates and current for 0.05Wt% Cu-TiO_2 electrode is shown in Fig. 6(a). The anodic peak current I_{pa} increased linearly with increasing scan rate which signifies the direct electron transfer between the electrode and surface diffusion controlled process [37-38]. Likewise the cathodic peak current I_{pc} decreases linearly with increase in scan rate. Fig. 6(b) shows the Linearity calibration plot for anodic current Vs scan rate, which is obtained by least square regression method. The regression equation is I_{pa} (A) = 2E-08x - 2E-07, with a correlation coefficient of 0.992.

The electrochemical response of 0.05Wt% Cu-TiO_2 electrode at 150mV/s Scan rate for 10 cycles is shown in Fig. 7. The stability of the electrode was observed with respect to the number of scanned cycles [39]. With increasing the number of cycles the CV sweep plot remain the same. It signifies that the 0.05Wt% Cu-TiO_2 electrode has good stability which may be used as electrode material to construct biosensors.

Electrochemical response of 0.05 Wt% Cu-TiO_2 for UA sensing

In the sensing process, UA was added in different concentrations ie; 1mM, 3mM, 5mM and 10 mM into 0.1M PBS electrolyte with 0.05 Wt% Cu-TiO_2 film as working electrode.

The comparison CV plot of sensing of different concentrations of UA in 0.1M PBS electrolyte with 0.05 Wt% Cu-TiO_2 electrode is shown in Fig. 8. It is observed from the plot that the 0.05 Wt% Cu-TiO_2 electrode shows a fast and sensitive response for UA. The anodic peak current has

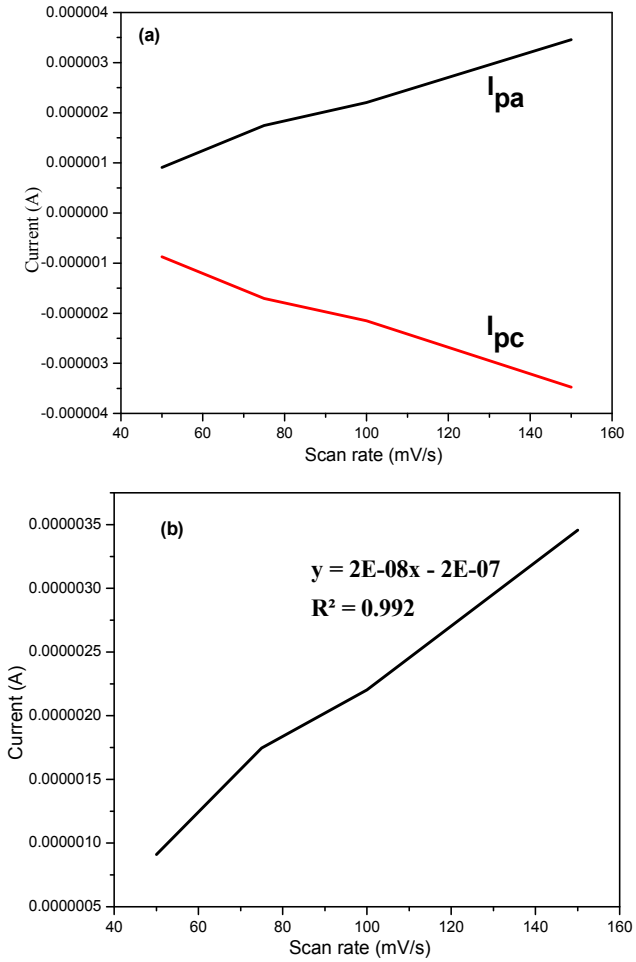

Fig. 6(a) & (b). Correlation between anodic & cathodic current Vs Scan rate for 0.05Wt% Cu-TiO_2 and linearity calibration plot for anodic current Vs Scan rate.

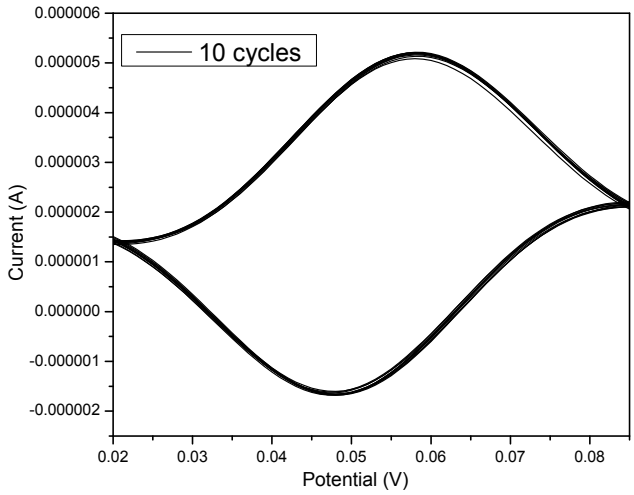

Fig. 7. Electrochemical response of 0.05 Wt% Cu-TiO_2 at scan rate of 150mV/s for 10 cycles.

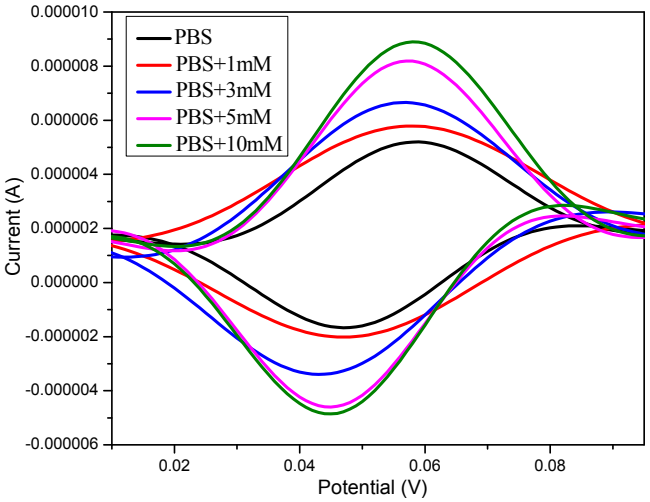

Fig. 8. Comparison CV sweep curve of 0.05 Wt% Cu-TiO_2 with different UA concentrations in 0.1M PBS.

Table 4. anodic and cathodic peak potential (E_{pa}, E_{pc}) & anodic and cathodic peak current (I_{pa}, I_{pc}) of various concentration of UA.

Sample	Concentration	E_{pa}	E_{pc}	I_{pa}	I_{pc}
0.05Wt% Cu-TiO_2	PBS	0.0563	0.0468	3.46E-06	-3.47E-06
	PBS + 1mM UA	0.0564	0.0463	3.81E-06	-3.67E-06
	PBS + 3mM UA	0.0568	0.0456	4.57E-06	-4.51E-06
	PBS + 5mM UA	0.0570	0.0449	5.57E-06	-5.57E-06
	PBS+10mM UA	0.0575	0.0446	7.09E-06	-7.03E-06

been increased and the cathodic peak current decreased upon the successive addition of UA. The current voltage response of 0.05 Wt% Cu-TiO_2 electrode in the presence of UA in PBS solution shows higher response in comparison with PBS solution. The anodic and cathodic peak potential and current are tabulated in Table 4. The linear curve for anodic and cathodic peak current Vs concentration of UA is shown in Fig. 9(a). It reveals that the anodic current increases and cathodic current decreases as the concentration of UA are increased. The excellent linear relationship between the peak current and the concentration of UA signifies that the 0.05Wt% Cu-TiO_2 electrode shows good response as a UA sensor.

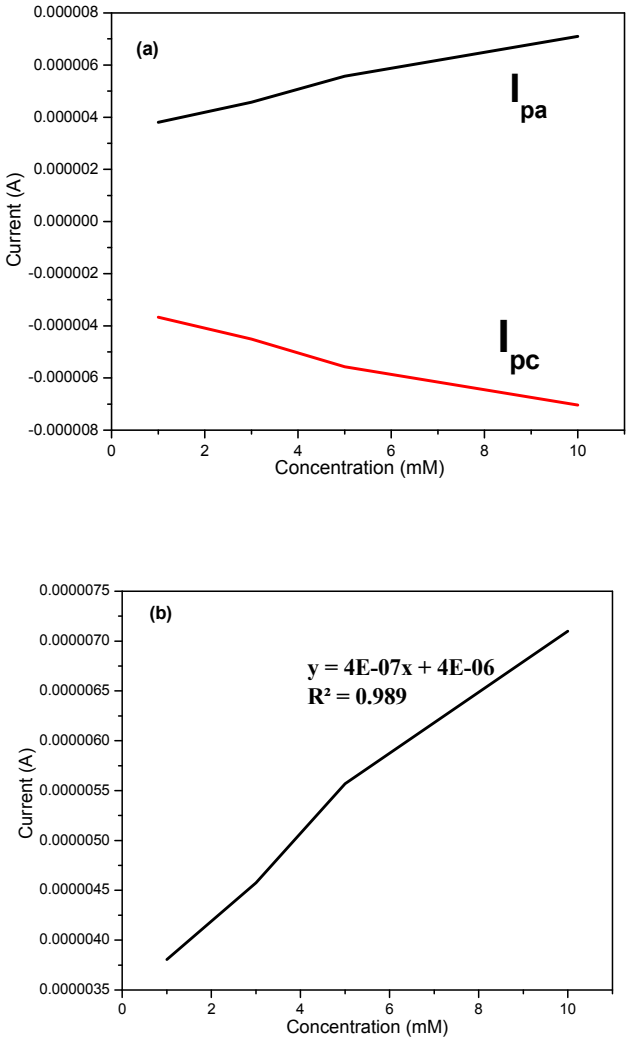

Fig. 9 (a),(b). anodic & cathodic current Vs concentration of UA and linearity calibration plot for anodic current Vs concentration of UA.

The linearity calibration plot for anodic current Vs concentration of UA, which was evaluated by least square regression method, is shown in Fig. 9(b). The regression equation for 0.05Wt% Cu-TiO_2 electrode with various concentration of UA is I_{pa} (µA) = 4E-07x + 4E-06 and its correlation coefficient is 0.989. The sensitivity of UA of 0.05 Wt% Cu-TiO_2 electrode as obtained from the above plot is 3.81µA $mM^{-1}cm^{-2}$. The linear range of UA detection is 1mM-10mM.

CONCLUSION

Uric acid (UA) biosensor was successfully constructed using Cu doped TiO_2 electrode in an electrochemical cell. TiO_2 thin films and Cu-TiO_2 thin films were effectively prepared by spray pyrolysis technique with different concentration of Cu. The XRD analysis reveals the anatase and also less intense rutile phases of the film with tetragonal structure. The crystalline size was highest and the dislocation density, strain, optical band gap and PL intensity were lowest for the 0.05Wt% Cu- TiO_2 sample. Good crystallinity and electrical, optical and surface properties of 0.05Wt% Cu TiO_2 film show that the film is good for fabrication of biosensor. The electrochemical response studies of Cu-TiO_2 electrode for detection of UA show high stability, with sensitivity of 3.81µA $mM^{-1}cm^{-2}$. The current study implies that the constructed Cu-TiO_2 thin film based electrochemical biosensor act as a potential candidate for application in the detection of UA.

CONFLICT OF INTEREST

The authors declare that there are no conflicts of interest regarding the publication of this manuscript.

REFERENCES

[1] Dryhurst G., (1977), Electrochemistry of Biological Molecules. *NewYork,* Academic Press.

[2] Zen J. M., Jou J. J., Ilangovan G., (1998), Selective voltammetric method for uric acid detection using pre-anodized Nafion-coated glassy carbon electrodes. *Analyst.* 123: 1345-1350.

[3] Özcan A., İlkbaş S., (2015), Preparation of poly (3, 4-Ethylenedioxythiophene) nanofibers modified pencil graphite electrode and investigation of over-oxidation conditions for the selective and sensitive determination of uric acid in body fluids. *Anal. Chim. Acta.* 891: 312-320.

[4] Yue H. Y., Zhang H., Chang J., Gao X., Huang S., Yao L. H., Lin X. Y., Guo E. J., (2015), Highly sensitive and selective uric acid biosensor based on a three-dimensional graphene foam/indium tin oxide glass electrode. *Anal. Biochem.* 488: 22–27.

[5] Dong W., Hai-Feng L., He X., Juan W., Cheng-Ming W., Qun-Lin Zh., (2015), Uricase stimulated etching of silver nanoprisms for highly selective and sensitive colorimetric detection of uric acid in human serum. *Sens. Actuators B: Chem.* 221: 1433–1440.

[6] Hongxiu D., Nan W., Donglei W., Xiaomei Zh., Houyi M., Meng L., (2016), Voltammetric uric acid sensor based on a glassy carbon electrode modified with a nanocomposite consisting of poly tetra phenyl porphyrin, polypyrrole, and graphene oxide. *Microchim. Acta.* 183: 3053-3059.

[7] Dai X., Fang X., Zhang C., Xu R., Xu B., (2007), Determination of serum uric acid using high-performance liquid chromatography (HPLC)/isotope dilution mass spectrometry (ID-MS) as a candidate reference method. *J Chromatogr. B. Analyt. Technol. Biomed. Life Sci.* 857: 287-295.

[8] Cete S., Yasar A., Arslan F., (2006), An amperometric biosensor or uric acid determination prepared from uricase immobilised in polypyrrole film. *Artif. Cells Blood Substit. Immobil. Biotechnol.* 34: 367-380.

[9] Jalban G., Andreu Y., Almenara M. J., De Marcos S., Castillo J. R., (2001), Direct determination of uric acid in serum by a fluorometric-enzymatic method based on uricase. *Talanta.* 54: 847-854.

[10] Rajabi H., Noroozifar M., Sabbaghi N., (2017), Electrochemical determination of Uric Acid using nano resin modified Carbon paste electrode as a new sensor. *J. Mater. Appl. Sci.* 1: 1002-1006.

[11] Abbasi A., Jahanbin Sardroodi J., (2016), A theoretical study on the adsorption behaviors of ammonia molecule on N-doped TiO_2 anatase nanoparticles: Applications to gas sensor devices. *Int. J. Nano Dimens.* 7: 349-359.

[12] Jinwen W., Guangqing X., Xu Zh., Jun L., Xinyi Zh., Zhixiang Zh., Yucheng W., (2015), Electrochemical performance and biosensor application of TiO_2 nanotube arrays with mesoporous structures constructed by chemical etching. *Dalton Transact.* 44: 7662-7672.

[13] Cui X., Li C. M., Zang J., Yu S., (2007), Highly sensitive lactate biosensor by engineering chitosan/PVI-Os/CNT/LOD network nanocomposite. *Biosen. Bioelectronics.* 22: 3288-3292.

[14] Zang J. F., Li C. M., Cui X. Q., Wang J. X., Sun X. W., Dong H., Sun C. Q., (2007), Tailoring zinc oxide nanowires for high performance amperometric glucose sensor. *Electro Analysis.* 19: 1008–1014.

[15] Vidhya R., Gandhimathi A., Neyvasagam M., (2017), Phtotocatalytic degradation of methyelene blue by Cu Doped TiO_2 thin films under visible light irradiation. *Mech. Mater. Sci. Eng. J. Magnolithe.* 9: 395-400.

[16] Suresh S., Pandurangan K., (2015), Investigations on structural and electrical properties of Cadmium Zinc Sulfide thin films. *Int. J. Nano Dimens.* 6: 433-438.

[17] Gowri manohari A., Dhanapandian S., Santhosh K., Mahalingam T., (2014), Optimization of deposition parameters on the physical properties of TiO_2 thin films by spray pyrolysis technique. *Int. J. Thin Fil. Sci. Tec.* 3: 1-6.

[18] Patil P. S., (1999), Versatility of chemical spray pyrolysis technique. *Mater. Chem. Phys.* 59: 185-198.

[19] Thanh Binh N., Moon-Jin H., Kwang-Sun R., (2012), Synthesis and high photocatalytic activity of Zn-doped TiO_2 nanoparticles by sol-gel and ammonia-evaporation method. *Bull. Korean Chem. Soc.* 33: 243-247.

[20] Ya-Fang T., Sheng-You H., Jian-Ping S., Xian-Wu Z., (2009), Synthesis and photocatalytic properties of Sn-doped TiO_2 nanotube arrays. *J. Alloy. Compd.* 482: 382–387.

[21] Linhua X., Hua Sh., Xiangyin L., Rihong Zh., (2010), Influence of annealing temperature on the photoluminescence property of ZnO thin film covered by TiO_2 nanoparticles. *J. Lumin.* 130: 2123–2127.

[22] Arunachalam A., Dhanapandian S., Manoharan C., (2016), Effect of Sn doping on the structural, optical and electrical properties of TiO_2 films prepared by spray pyrolysis. *Physica E.* 76: 35-46.

[23] Wang R., Sakai N., Fujishima A., Watanabe T., Hashimoto K., (1999), Studies of surface wettability conversion on TiO_2 single-crystal surfaces. *J. Phys. Chem. B.* 103: 2188-2194. .

[24] Ruby Ch., Ashavani K., Ram Pal Ch., (2012), Structural and optical characterization of Zn doped TiO_2 nanoparticles prepared by sol–gel method. *J. Sol-Gel Sci. Technol.* 61: 585–591.

[25] Tim L., Sandamali H., Junguang T., Alan K., Eli S., Matthias B., (2014), Why is anatase a better photocatalyst than rutile? Model studies on epitaxial TiO_2 films. *Scientif. Reports.* 4: 4043-4047.

[26] Senthilkumar V., Jayachandran M., Sanjeeviraja C., (2010), Preparation of anatase TiO_2 thin films for dye-sensitized solar cells by DC reactive magnetron sputtering technique. *Thin Solid Films.* 5: 991–994.

[27] Madan S., Monika G., Kamal D., (2018), Size and shape effects on the band gap of semiconductor compound nanomaterials. *J. Taibah Univ. Sci.* 4: 470-475.

[28] Pattanasak T., Orawan W., Wonchai P., (2017), Preparation and characterization of copper doped titanium dioxide thin film by sparking process. *SNRU J. Sci. Technol.* 9: 583-591.

[29] Jianping X., Shaobo Sh., Lan L., Xiaosong Zh., Yaxin W., Ximing Ch., Jianfeng W., Liya L., Fengming Zh., Wei Zh., (2010), Structural, optical, and ferromagnetic properties of Co-doped TiO_2 films annealed in vacuum. *J. Appl. Phys.* 107: 053910.

[30] Kim T. W., Lee D. U., Yoon Y. S., (2000), Microstructural, electrical, and optical properties of SnO_2 nanocrystalline thin films grown on InP (100) substrates for applications as gas sensor devices. *J. Appl. Phys.* 88: 3759-3764.

[31] Prabitha B., Justinvictor V. B., Daniel G. P., Joy K., Ramakrishnan V., Kumar D. D., Thomas P. V., (2014), Structural, optical, photoluminescence and photocatalytic investigations on Fe doped Tio_2 thin films. *Thin Solid Films.* 550: 121–127.

[32] Neha B., Monika T., Prateek J., Vinay G., (2013), Laser ablated ZnO thin film for amperometric detection of urea. *J. Appl. Phys.* 114: 124702.

[33] Liangsheng H., Kaifu H., Rongsheng Ch., Biao G., Jijiang F., Paul Ch., (2011), Recyclable and high-sensitivity electrochemical biosensing platform composed of Carbon-doped TiO_2 nanotube arrays. *Anal. Chem*. 83: 8138-8144.

[34] Wang S., Meng K. K., Zhao L., Jiang Q., Lian J. S., (2014), Superhydrophilic Cu-doped TiO_2 thin film for solar- driven photocatalysis. *Ceram. Int.* 40: 5107-5110.

[35] Zhenguang Sh., Zengying Zh., Jian W., Jingwen Q., Zhijian P., Xiuli F., (2018), Role of oxygen vacancies in the electrical properties of WO_{3-x} nano/microrods with identical morphology. *Hindawi J. Nanomater.* 2018: Article ID 7802589, 12 pages.

[36] Al-Furjan M. S. H.., Kui Ch., WenjianW., (2014), Influences of Mg doping on the electrochemical performance of TiO_2 nanodots based biosensor electrodes. *Adv. Mater. Sci. Eng.* 2014: Article ID 965821, 8 pages.

[37] Ansari A. A., Solanki P. R., Malhotra B. D., (2009), Hydrogen peroxide sensor based on horseradish peroxidase immobilized nanostructured cerium oxide film. *J. Biotechnol.* 142: 179-184.

[38]. Teng Y. J., Zuo S. H., Lan M. B., (2009), Direct electron transfer of horseradish peroxidase on porous structure of screen-printed electrode. Biosens. Bioelectron. 24: 1353-1357.

[39] Jinwen W., Guangqing X., Xu Zh., Jun L., Xinyi Zh., Zhixiang Zh., Yucheng W., (2015), Electrochemical performance and biosensor application of TiO_2 nanotube arrays with mesoporous structures constructed by chemical etching. *Dalton Trans.* 44: 7662-7672.